Available online at www.sciencedirect.com
SCIENCE DIRECT®
Journal of Power Sources 130 (2004) 129–135
JOURNAL OF POWER SOURCES
www.elsevier.com/locate/jpowsour

Assessment of ceramic membrane reforming in a solid oxide fuel cell stack

A. Atkinson*, T. Ramos

Department of Materials, Imperial College London, Exhibition Road, London SW7 2BP, UK

Received 3 August 2003; received in revised form 27 November 2003; accepted 29 November 2003

Abstract

Partial oxidation reforming of methane using a ceramic mixed ionic (oxygen)/electronic conducting dense ceramic membrane within a solid oxide fuel cell (SOFC) stack is potentially attractive as it allows direct operation on methane. We have analysed this process using a simple model of a counter-flow fuel system in which steam and carbon dioxide from the anode channel of the SOFC provide oxygen which passes through the mixed conducting membrane to partially oxidise methane on the other side of the membrane. The model shows that the concept is feasible and that the efficiency is the same as direct methane operation. The model also gives target values for the properties of the membrane. Tracer oxygen diffusion and exchange have been measured in the family of oxides $La_{1-x}Sr_xFe_{0.8}Cr_{0.2}O_{3-\delta}$ under reducing conditions. The data show that these materials have the mass transport characteristics and stability required for this concept.

Keywords: Solid oxide fuel cell; Reforming; Perovskite; Ceramic membrane; Modelling

1. Introduction

Ideally, fuel cells should be able to run directly on the raw fuel of choice, but this is currently not feasible for SOFCs fuelled by natural gas (mainly methane). There has been some success with direct methane operation using ceria-based anodes [1,2], but there are still significant problems with the high anode over-voltage and carbon deposition. Consequently, it is usual to reform the methane to H_2 and CO before electrochemical oxidation at the anode. Internal steam reforming on the anodes is the most desirable, but the amount of steam required to suppress carbon deposition is much greater than the 1:1 steam:methane ratio required for the reforming reaction. The extra steam absorbs energy (reducing efficiency), dilutes the anode reactions (reducing power density) and increases balance-of-plant complexity (raising steam and/or recycling it). Furthermore, the rapid endothermic reforming reaction on the first few anodes of the stack gives a large cooling effect which reduces output and can cause mechanical degradation, particularly with ceramic structures [3]. External steam reforming or in-stack reforming are more controllable, but again require excess steam and lead to a loss in efficiency unless there is very good transfer of heat from the cell reaction to the reforming reaction. Partial oxidation reforming requires no added steam, but reduces efficiency considerably.

Several suggestions have been made to overcome these problems. For example, a concept of gradual internal reforming has been proposed to avoid the cooling of the first anodes [4]. However, this is still potentially susceptible to carbon deposition. As an alternative, Steele [5] suggested using the steam and CO_2 created by the SOFC cell reaction to partially oxidise the methane feed by transfer of oxygen through a dense oxygen-permeable ceramic membrane. The transfer would simultaneously boost the H_2 and CO concentrations in the anode stream and thereby increase the output of the cells. Membrane reforming of methane by partial oxidation of oxygen from air is an area of great interest in its own right and oxides with suitable properties are being developed [6] that could be adapted for application in SOFCs. The work described here has two objectives. The first is to show by a modelling approach that membrane reforming of methane in a SOFC is feasible in principle. The second is to identify potential membrane materials that have the required thermo-chemical stability and transport properties.

* Corresponding author. Tel.: +44-207-5946780; fax: +44-207-5946780.
E-mail address: alan.atkinson@imperial.ac.uk (A. Atkinson).

0378-7753/$ – see front matter © 2003 Elsevier B.V. All rights reserved.
doi:10.1016/j.jpowsour.2003.11.047

Nomenclature

A_S	area of a reaction site
c_O	concentration of oxygen in solid phase
C, $C_{a,i}$, $C_{r,i}$	molar reformate concentration in ith cell of anode or reformer channel
C_T	total volumetric molar gas concentration
D^*	oxygen tracer diffusion coefficient
F	Faraday's constant
F_a	gas velocity in anode channel
$F_{r,i}$	gas velocity in ith cell of reformer channel
h	height of reformer and anode channels
i_c, i_m	current densities in fuel cells and reformer membrane
j_O	oxygen flux density
k_1, k_2	interfacial exchange coefficients (rate constants) at membrane surfaces
K_a, K_r	equilibrium constants for gas in anode and reformer channels
l	length of each fuel cell
L	membrane thickness
N_A	Avagadro's number
N_O	number of moles of oxygen
N_r	turnover frequency for reformer reaction with methane
P_a, P_r	oxygen activities in anode and reformer channels
$P_{O_2,1}$, $P_{O_2,2}$	oxygen activities at membrane surfaces
r_c, r_m	area-specific resistances of fuel cells and reformer membrane
R	gas constant
t	time
T	temperature
V_{MO}	volume of oxide per gram atom of oxygen
V_N	Nernst potential
w	width of each fuel cell
Greek letters	
γ	thermodynamic factor for oxygen in solid phase
μ_O	chemical potential of oxygen atoms

2. Transport through a mixed conducting ceramic membrane

The overall rate of permeation of oxygen through the membrane is controlled by reaction at the two membrane surfaces and the transport of oxygen ions and electrons through the membrane. The membrane material must be a mixed ionic and electronic conductor with a high oxygen ion conductivity. For materials in which the electronic conductivity is much greater than the ionic conductivity the steady state oxygen flux density (oxygen atoms per unit area per unit time) through a membrane of thickness L, is given by the expression [5]

$$j_O = \frac{N_A}{2V_{MO}} \frac{\ln(P_{O_2,1}/P_{O_2,2})}{(L/\langle D^* \rangle) + (1/k_a) + (1/k_c)} \quad (1)$$

where

$$\langle D^* \rangle = \frac{\int_a^c D^* \, d(\ln P_{O_2})}{\int_a^c d(\ln P_{O_2})} \quad (2)$$

and N_A is Avagadro's number. k_a and k_c are the surface reaction rate constants ($m\,s^{-1}$) for the anodic and cathodic interfacial reactions of oxygen at the membrane surfaces defined by the following equation [7,8]:

$$j\,(\text{O atoms equivalent}) = k \frac{N_A}{V_{MO}} \frac{\Delta\mu_O}{RT} \quad (3)$$

In these expressions the subscripts 1 and 2 denote the gas phases on the two sides of the membrane and a and c are the anodic and cathodic reaction surfaces of the solid membrane. The activities of molecular oxygen at these interfaces are not equal to those of the corresponding gas phases because of the chemical driving force of the interface reactions. This is accounted for by the drop in atomic oxygen chemical potential, $\Delta\mu_O$, in going from the gas to the solid. (Note that $\Delta\mu_O = (1/2)\Delta\mu_{O_2}$ for molecular oxygen.) V_{MO} is the volume of the oxide per gram atom of oxygen (and is approximately 12.1 cm^3 for the doped $LaFeO_3$ oxides discussed later).

The membrane can also be regarded as an equivalent electrical circuit in which the electro-motive force is the Nernst potential, V_N, of the two gaseous oxygen activities

$$V_N = \frac{RT}{4F} \ln\left(\frac{P_{O_2,1}}{P_{O_2,2}}\right) \quad (4)$$

and the current is carried by the oxygen ions. The equivalent area-specific resistance of the membrane is then given by

$$r_m = \left(\frac{1}{\langle D^* \rangle} + \frac{1}{k_1} + \frac{1}{k_2}\right) \frac{V_{MO} RT}{4F^2} \quad (5)$$

3. Membrane reforming in the SOFC

In order to evaluate the concept we have constructed a simple SOFC model with an integrated ceramic membrane reformer. The model uses simplified descriptions of the electrochemical and transport phenomena. It is recognised that in reality these processes are much more complicated, but nevertheless they serve to illustrate the coupling between the SOFC cells and the membrane reformer. Fig. 1 shows the model used. It consists of 20 planar cells connected in series such that the current is the same in each cell and the cell potential is different for each cell. This configuration is similar to the "segmented in series" design [9,10]. (Although

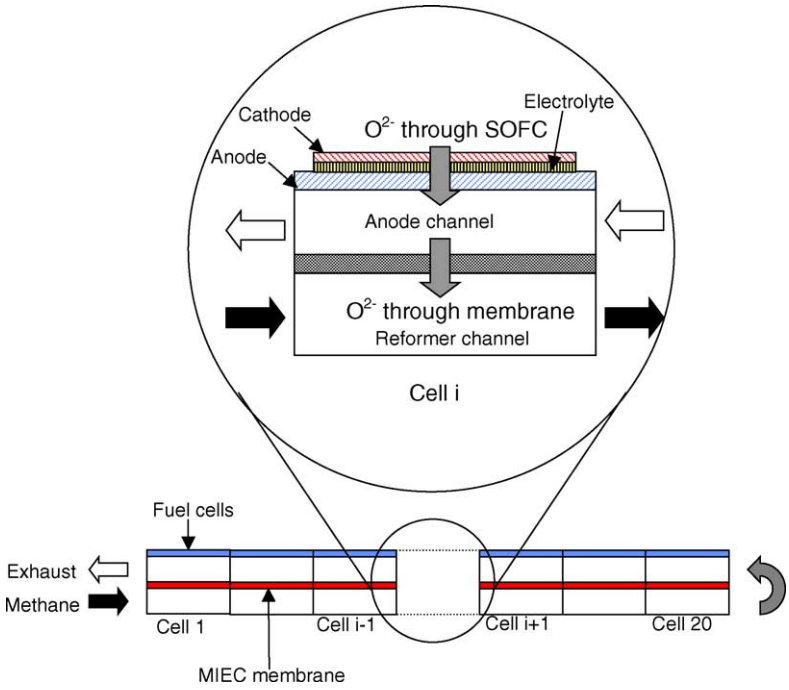

Fig. 1. The SOFC and membrane configuration used in the model.

we consider a specific SOFC configuration in the model, this is only to illustrate the membrane reforming concept. The broad conclusions should be applicable to other geometries.) Methane enters the reformer channel and is reformed by partial oxidation by oxygen diffusing through the membrane from the anode channel. The partial reactions at the two surfaces of the membrane are

$$H_2O + 2e^- \rightarrow O^{2-} + H_2 \quad \text{and}$$
$$CO_2 + 2e^- \rightarrow O^{2-} + CO \tag{6}$$

in the anode channel and

$$CH_4 + O^{2-} \rightarrow CO + 2H_2 + 2e^- \tag{7}$$

in the reformer channel.

At the end of the reformer channel the reformate stream is reversed into the anode channel of the fuel cells. The flow of oxygen through each fuel cell into its anode channel is given by the cell current density i_c and the cell potential of each cell by

$$V_{cell} = V_{N,c} - i_c r_c \tag{8}$$

where r_c is the area-specific resistance (ASR) of the fuel cells. This assumes that the polarisation of the electrodes is linear.

The flow of oxygen across the reformer membrane is driven by the difference in oxygen activities between the anode compartment and the reformer compartment of each cell. The equivalent electrical current is given by

$$i_m = \frac{V_{N,m}}{r_m} \tag{9}$$

where $V_{N,m}$ is the Nernst potential across the membrane and the ASR of the membrane is given by Eq. (5).

The mass balance equations for each cell include the material entering and leaving the cell by advective flow and the oxygen entering and leaving across the fuel cells and the membrane. Each cell is assumed to have no gradients other than through its thickness and therefore a finite element approach is used. The moles of oxygen ions crossing each fuel cell per unit time is

$$\left(\frac{\partial N_O}{\partial t}\right)_c = \frac{wl}{2F} i_c \tag{10}$$

where w is the width of a cell and l its length. The corresponding number crossing the MIEC membrane is

$$\left(\frac{\partial N_O}{\partial t}\right)_m = \frac{wl}{2F}\frac{1}{r_m}\frac{RT}{4F}\ln\left(\frac{P_a}{P_r}\right) \tag{11}$$

where P_a and P_r are the oxygen activities in the anode and reformer sections of the cell.

Thermodynamic equilibrium is assumed locally in each cell. Gas equilibrium calculations [11] indicate that the ratio of H_2 to CO should be approximately 2 throughout both the reformer and anode channels (when C deposition is suppressed). Therefore, in order to simplify the model, it is permissible to treat the reformate mixture as though it were all H_2, but at an effective reformate concentration equal to 1.5 times the true H_2 concentration. Thus the mass balance for the reformate concentration (C moles per unit volume) in the anode channel of the ith cell gives

$$\frac{dC_{a,i}}{dt} = \frac{F_a}{l}(C_{a,i+1} - C_{a,i}) - \frac{i_c}{2Fh} + \frac{RT}{8F^2 h r_m}\ln\left(\frac{P_a}{P_r}\right) \tag{12}$$

In this equation F_a is the linear flow velocity in the anode channel and h is the height of the channel. The flow velocity is constant in the anode channel because both the fuel cell anode reaction and the membrane reaction conserve the number of gas molecules. The first term in Eq. (12) is the advective contribution (bearing in mind the reversed gas flow means that it is flowing from high to low cell indices), the second term is consumption of reformate by the fuel cell reaction and the third term is increase in reformate concentration by loss of oxygen through the MIEC membrane. The corresponding mass balance for the reformer channel is

$$\frac{dC_{r,i}}{dt} = \frac{1}{l}(F_{r,i-1}C_{r,i-1} - F_{r,i}C_{r,i}) + \frac{3RT}{8F^2hr_m}\ln\left(\frac{P_a}{P_r}\right) \quad (13)$$

The first term is again the advective contribution, but this is slightly more complicated because the flow velocity in the reformer channel is not constant because the reforming reaction increases the number of gas molecules. The second term is due to oxygen permeating the MIEC membrane and the factor of 3 is because each oxygen atom passing through the membrane produces three molecules of reformate (Eq. (7)). The increase in reformate flow velocity at each cell is given by

$$F_{r,i} - F_{r,i-1} = \left(\frac{RT}{4F}\right)^2 \frac{4l}{Phr_m}\ln\left(\frac{P_a}{P_r}\right) \quad (14)$$

where P is the total pressure. The anode flow velocity is equal to the reformer flow velocity in the last cell ($i = 20$) because the output of the reformer is delivered into the anode channel at this cell.

Gas phase equilibrium in the anode channels is determined by the reactions:

$$H_2 + \tfrac{1}{2}O_2 \leftrightarrow H_2O \quad (15)$$

and

$$CO + \tfrac{1}{2}O_2 \leftrightarrow CO_2 \quad (16)$$

Since these have similar free energy changes (−182,944 kJ for Eq. (15) and −180,424 kJ for Eq. (16) [11]) then we can approximate them as being equal (this is why the reformate retains stoichiometric composition). Thus the equilibrium oxygen activity in the anode channel can be described by the following equation:

$$P_a = \left(\frac{C_T - C}{K_a C}\right)^2 \quad (17)$$

where C_T is the total number of gas moles per unit volume at a pressure of 1 atm (10.25 m^{-3}) and K_a is the equilibrium constant for Eq. (15) (= 1.4×10^8 at 900 °C [11]).

Gas phase equilibrium in the reformer channel is controlled by the reaction

$$CH_4 + \tfrac{1}{2}O_2 \rightarrow CO + 2H_2 \quad (18)$$

Assuming stoichiometric conversion then the concentration of CO is $C/3$ and that of H_2 is $2C/3$. Equilibrium of Eq. (16) then gives the oxygen activity in the reformer channel as

$$P_r = \left\{\frac{4C^3}{27K_rC_T^2(C_T - C)}\right\}^2 \quad (19)$$

where K_r is the equilibrium constant for Eq. (16) (=1.93×10^{11} at 900 °C [11]).

The initial condition employed to give a stable start was that all the reformer and anode channels were initially filled with a mixture of reformate with 10% CH_4 and the CH_4 was not allowed to react in the fuel cells. For $t > 0$ the input to the reformer channel was 99.9% CH_4 and 0.1% reformate at constant flow rate. The cathodes were assumed to be in equilibrium with air at atmospheric pressure. Eqs. (12) and (13) were solved numerically by finite difference time step (typically one-tenth of the residence time per cell) using Maple software (Waterloo Maple Inc.). The simulations were carried out for a constant temperature of 900 °C, pressure of 1 atm, cell ASR of 0.5 Ω cm^2 and fuel utilisation of approximately 85%. Each cell was assumed to have width of 100 mm and length in the flow direction of 20 mm. The heights of the reformer and anode channels were both taken to be 5 mm. The simulations were run until they reached steady state. In order to provide a comparison, a simulation was also carried out with stoichiometric external steam reforming (and no membrane reforming).

The input flow velocity and the MIEC membrane ASR were then adjusted to achieve close to full methane conversion at the end of the reformer channel and 85% fuel utilisation. This is a limiting case since if conversion is incomplete, unreformed methane will enter the fuel cell anodes, leading to a risk of carbon deposition on the anodes. The reformate profiles in the reformer and anode channels are shown in Fig. 2. The reformate fraction is defined as the sum of the mole fractions of H_2 and CO in the gas stream. The model demonstrates that a stable steady state exists to achieve approximately complete membrane reforming and for this particular case, the ASR of the membrane should be less than 7 Ω cm^2. Most of the reforming takes place within the first one-third of the reformer channel. Also shown in Fig. 2 is the reformate concentration profile in the anode channel for external reforming. This is strictly linear because the constant cell current removes reformate at a constant rate. The corresponding anode profile for membrane reforming shows a slight curvature caused by the membrane increasing the reformate concentration in the anodes of the low index cells.

Fig. 3 shows the oxygen activity profiles in the reformer and anode channels. It is the difference between them that drives permeation through the reformer membrane. The difference is largest for the lower index cells, which is consistent with most of the reforming being performed in these cells. The oxygen activity profiles in the anode are very similar for both the membrane and external reforming cases, as is expected from the similarity in the reformate profiles in

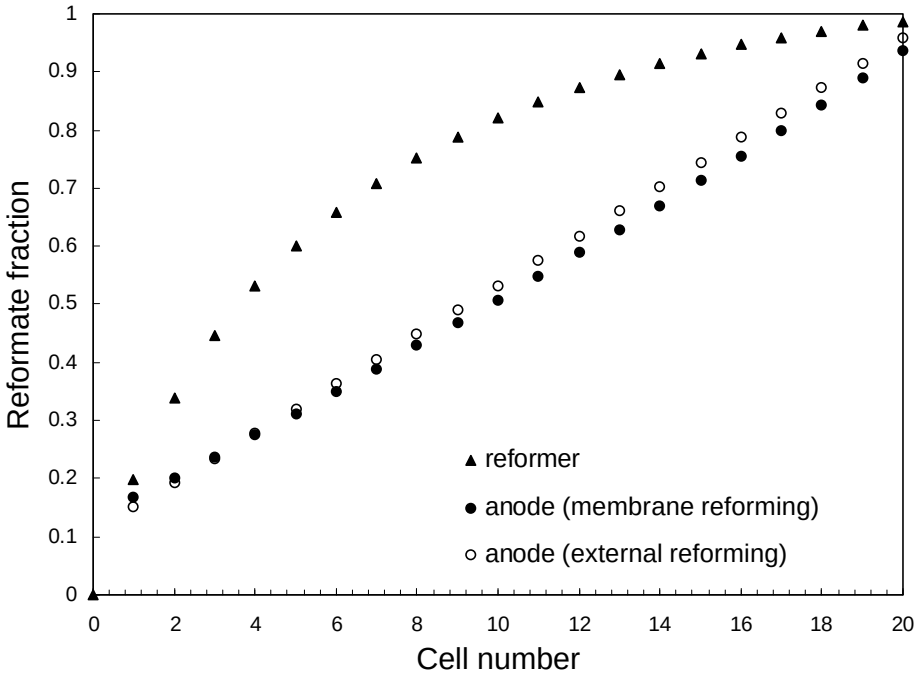

Fig. 2. Profiles of the fraction of reformate in the gas stream in the reformer channel and the anode channel calculated from the membrane reformer model at the critical membrane ASR of $7\,\Omega\,cm^2$ (cell current density: $0.25\,A\,cm^{-2}$, temperature: 900 °C, fuel utilisation: 85%). Also shown is the profile in the anode channel for external steam reforming under the same conditions.

Fig. 2. The cell voltage profiles are also shown in Fig. 3 and there is no detectable difference between the membrane and external reforming cases. The driving force for transport across the reformer membrane can be expressed as an electro-motive force given by applying the Nernst equation to the ratio of oxygen partial pressures on the two sides of the membrane. This is also shown as a function of cell number in Fig. 3.

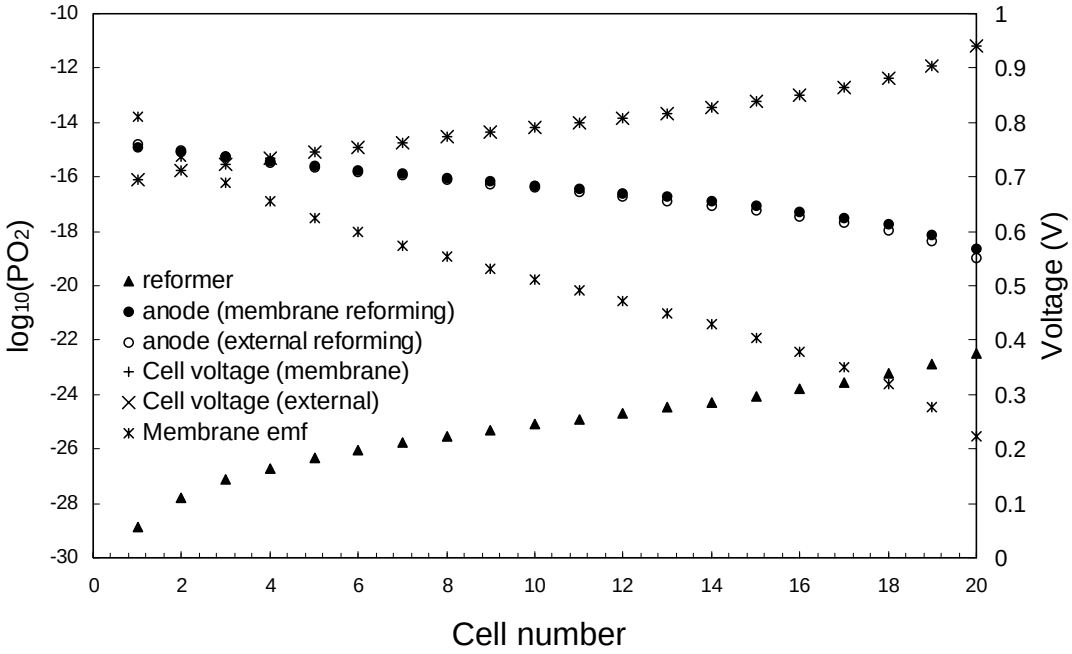

Fig. 3. Profiles of oxygen activity in the reformer channel and the anode channel calculated from the membrane reformer model at the critical membrane ASR of $7\,\Omega\,cm^2$ (cell current density: $0.25\,A\,cm^{-2}$, temperature: 900 °C, fuel utilisation: 85%). Also shown is the profile in the anode channel for external steam reforming under the same conditions, the cell voltage profile for both conditions (these are indistinguishable) and the Nernst emf across the membrane.

Table 1
Summary of calculations comparing a SOFC with membrane reforming with one having external steam reforming

Parameter	External reforming	Membrane reforming
Membrane ASR ($\Omega\,cm^2$)	N/A	7
Fuel utilisation (%)	84.2	84.9
Electrical efficiency (% LHV)	48.2	62.4
Total voltage (V)	16.0	15.89
Fuel input velocity ($m\,s^{-1}$)	0.119	0.031
Exhaust output velocity ($m\,s^{-1}$)	0.119	0.0892

Operating temperature: 900 °C, current density: 0.25 $A\,cm^{-2}$, SOFC ASR: 0.5 $\Omega\,cm^2$.

The electrical efficiency was calculated for the SOFC with membrane reformer, the output electrical power divided by the room temperature LHV of the input methane ($\Delta H^{\circ}_{298} = -802,286\,J\,mol^{-1}$ [11]). This was also done for the external reforming base case. The results are shown in Table 1. The membrane reforming increases the efficiency for electrical power generation from 48.2 to 62.4%. This is entirely due to the fact that the internal membrane reforming essentially converts the SOFC to direct methane operation. The lower efficiency of external steam reforming is due to the enthalpy requirement of the steam reforming reaction. If all this enthalpy could be extracted from the waste heat of the SOFC then the efficiency for steam reforming would increase to that of the membrane reforming case. Since internal steam reforming should be able to achieve this, there is no efficiency advantage of membrane reforming over internal steam reforming, but membrane reforming removes the other problems associated with on-anode steam reforming.

4. Potential membrane material

The family $La_{1-x}Sr_xFe_{1-y}Cr_yO_3$ (abbreviated as LSFCr) contains potentially suitable MIEC compositions whose stability, mass transport and interfacial reaction rates can be adjusted by changing x and y [12,13]. Increasing x or decreasing y increases mass transport, but reduces stability (both chemical and mechanical). The best compromise was found to be with $y = 0.2$ and x in the range 0.4–0.6. Oxygen tracer diffusion coefficients and isotopic surface exchange constants measured under reducing conditions similar to those predicted for membrane reforming are summarised in Fig. 4 [14]. At 900 °C and under reducing conditions the oxygen tracer diffusion coefficient is approximately $10^{-7}\,cm^2\,s^{-1}$ and is relatively insensitive to oxygen activity [15]. Thus the integration in Eq. (2) is not necessary. From Eq. (3) for a membrane thickness of 0.5 mm this tracer diffusion coefficient is equivalent to a contribution of 1.6 $\Omega\,cm^2$ to the ASR. Since the target value is $<7\,\Omega\,cm^2$, diffusion in these materials is sufficiently fast for this application.

Under the same conditions the surface isotopic exchange rate constant with H_2O/H_2 (k^*) is in the range 3×10^{-7} to $10 \times 10^{-7}\,cm\,s^{-1}$ at a water vapour pressure of 0.1 atm. The reaction rate constant is related to the tracer exchange constant by [16]

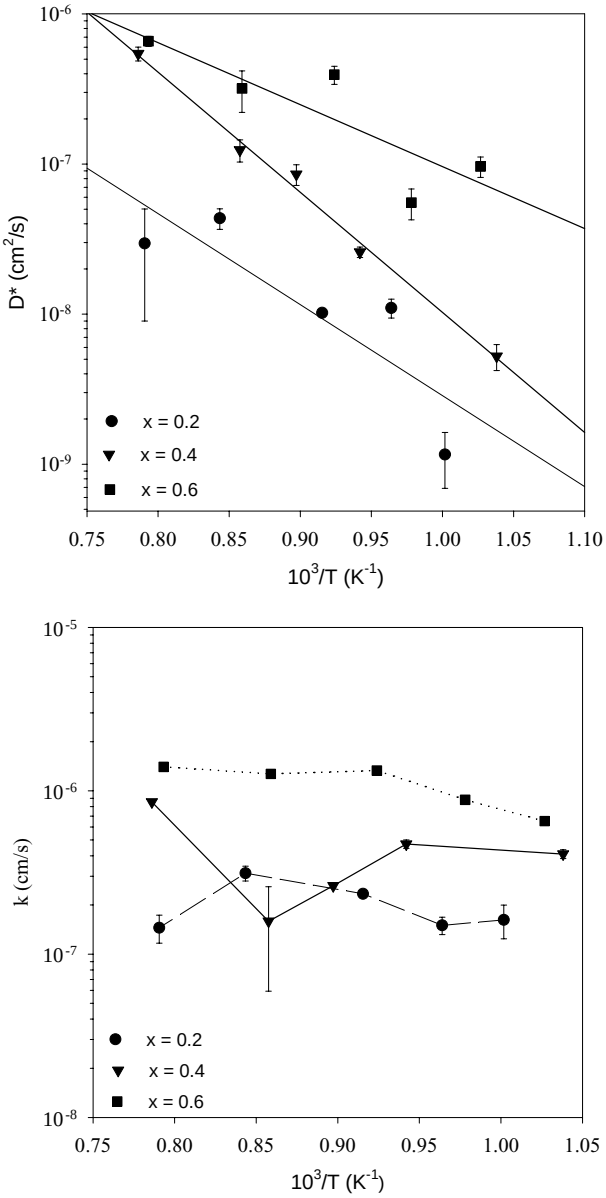

Fig. 4. D^* and k measured for LSFCr compositions in a gas composition of 0.05 atm H_2, 0.15 atm N_2, 0.1 atm H_2O.

$$k = k^* \left(2n + \frac{1}{\gamma}\right) \tag{20}$$

where n is the order of reaction for the gaseous species. γ is a thermodynamic factor

$$\gamma = \frac{1}{2}\frac{d(\ln P_{O_2})}{d(\ln c_O)} \tag{21}$$

where c_O is the concentration of oxygen in the solid phase. The dependence of k^* on water vapour pressure is not known, but could be linear i.e. $n = 1$ (it is assumed to be independent in the model). Similarly, γ is not known but is likely to

be $\gg 1$ in the region where D^* is independent of oxygen activity. Thus Eq. (20) reduces to $k \cong 2k^*$. The water vapour pressure varies along the anode channel, but that used in the measurements (0.1 atm) is a typical value. Hence from Eq. (5) the contribution to the membrane ASR from the cathodic reaction with water is in the range 1.6–5.3 $\Omega\,cm^2$ at 900 °C.

At the surface of the membrane with the reformer channel the anodic reaction parameter k_a is the reaction rate constant for oxidation of methane by LSFCr. The turnover frequency, N_r, for this reaction has been measured to be approximately three molecules of CH_4 per site per second at 5% methane and 900 °C [17]. The experiments also showed that these materials are extremely resistant to carbon deposition even when exposed directly to dry methane. The rate constant, as defined by Eq. (3), is related to the turnover frequency by

$$k_a = \frac{N_r V_{MO}}{N_A A_S} \frac{RT}{\Delta\mu_O} \tag{22}$$

where A_S is the area of a site measured by nitrogen adsorption ($1.62 \times 10^{-19}\,m^2$). The difference in oxygen chemical potential driving the reaction in the measurements of N_r was not known, but the driving force was large and probably beyond the limit of linear behaviour on which Eq. (3) is based. In order to make an approximate estimate, we therefore assume the factor $RT/\Delta\mu_O$ to be of order unity. The turnover frequency is proportional to the methane concentration (although assumed independent in the model) and in the reformer channel this is approximately 0.5 atm which is 10× that used in the measurement of N_r. Hence N_r for the anodic membrane reaction is approximately $30\,s^{-1}$ per site and the corresponding value of k_a for methane oxidation is thus $3.7 \times 10^{-7}\,cm\,s^{-1}$. From Eq. (5) this gives a contribution to the membrane ASR of 8.6 $\Omega\,cm^2$.

The total membrane ASR is thus approximately in the range 12–16 $\Omega\,cm^2$ which is about double the target value from the membrane reformer model. The experimental data indicate that the surface reactions dominate the equivalent resistance of the membrane and that the largest equivalent resistance is probably the reaction with methane. Thus, the membrane surfaces are likely to require catalytic coatings to increase the interfacial reaction rates. However, the required increases are modest (less than an order of magnitude) and this could probably be achieved by using a porous coating of the same LSFCr membrane material.

5. Conclusions

A simplified reaction model has shown that in-stack membrane reforming in a SOFC is conceptually feasible. Membrane reforming has the same efficiency as operating the SOFC directly on dry methane, but with much less risk of carbon deposition. It also avoids the complications of raising steam and anode cooling encountered with conventional on-anode steam reforming. The simulations indicate an increase in electrical efficiency of approximately 14 percentage points with respect to external steam reforming at the same fuel utilisation. For a fuel cell ASR of 0.5 $\Omega\,cm^2$, the membrane should have an ASR of less than 7 $\Omega\,cm^2$.

Experimental measurements of oxygen diffusion and surface reaction show that materials in the family $La_{1-x}Sr_xFe_{1-y}Cr_yO_3$ have sufficiently fast oxygen diffusion under reducing conditions to meet the target ASR. However, the surface reaction rates (especially oxidation of methane at the reformer surface of the membrane) are probably too low by about a factor of 2. The rates could be increased by using porous coatings of the same material on the membrane surfaces in order to meet the target.

Acknowledgements

The authors are grateful to EPSRC and the Link Applied Catalysis Program for financial support under grant GR/M05928. T. Ramos is also grateful to FCT-Programa Praxis XXI (Portugal) for the award of a study scholarship.

References

[1] H. Kim, C. Lu, W.L. Worrell, J.M. Vohs, R.J. Gorte, J. Electrochem. Soc. 149 (2002) A247.
[2] T. Hibino, S.Q. Wang, S. Kakimoto, M. Sano, Solid State Ionics 127 (2000) 89.
[3] P. Aguiar, E. Ramírez-Cabrera, N. Laosiripojana, A. Atkinson, L.S. Kershenbaum, D. Chadwick, Stud. Surf. Sci. Catal. 145 (2003) 387.
[4] P. Vernoux, M. Guillodo, J. Fouletier, A. Hammou, Solid State Ionics 135 (2000) 425.
[5] B.C.H. Steele, in: H.L. Tuller (Ed.), Oxygen Ion and Mixed Conductors and Their Technological Applications, Kluwer Academic Publishers, Dordrecht, 2000, p. 323.
[6] U. Balachandran, J.T. Dusek, R.L. Mieville, R.B. Poeppel, M.S. Kleefisch, S. Pei, T.P. Kobylinski, C.A. Udovich, A.C. Bose, Appl. Catal. A: General 133 (1995) 19.
[7] J.E. tenElshof, M.H.R. Lankhorst, H.J.M. Bouwmeester, J. Electrochem. Soc. 144 (1997) 1060.
[8] S. Kim, Y.L. Yang, A.J. Jacobson, B. Abeles, Solid State Ionics 121 (1999) 31.
[9] E.F. Sverdrup, C.J. Warde, R.L. Eback, Energy Conv. 13 (1973) 129.
[10] F.J. Gardner, M.J. Day, N.P. Brandon, M.N. Pashley, M. Cassidy, J. Power Sour. 86 (2000) 122.
[11] HSC Chemistry v4, Outokumpu, Pori, Finland.
[12] W.T. Stephens, T.J. Mazanec, H.U. Anderson, Solid State Ionics 129 (2000) 271.
[13] A. Atkinson, T. Ramos, Solid State Ionics 129 (2000) 259.
[14] T. Ramos, A. Atkinson, in: T.A. Ramanarayanan, W.L. Worrell, M. Mogensen (Eds.), Ionic and Mixed Conducting Ceramics IV, Electrochemistry Society, 2001.
[15] T. Ramos, Ph.D. Thesis, Imperial College, London, 2002.
[16] S. Kim, Y.L. Yang, A.J. Jacobson, B. Abeles, Solid State Ionics 121 (1999) 31.
[17] E. Ramirez-Cabrera, Ph.D. Thesis, Imperial College, London, 2001.